

From (+)-epigallocatechin gallate to a simplified synthetic analogue as a cytoadherence inhibitor for *P. falciparum*†

Cite this: *RSC Adv.*, 2014, 4, 4769

Sandra Gemma,^{abc} Simone Brogi,^{abc} Pradeep R. Patil,^{abc} Simone Giovani,^{abc} Stefania Lamponi,^{abc} Andrea Cappelli,^{abc} Ettore Novellino,^{ad} Alan Brown,^e Matthew K. Higgins,^f Khairul Mustafa,^g Tadge Szeszak,^{‡g} Alister G. Craig,^g Giuseppe Campiani,^{*abc} Stefania Butini^{abc} and Margherita Brindisi^{abc}

Parasite derived surface antigen PfEMP1 is a virulence factor of the human malaria parasite. PfEMP1 variants have been implicated in the cytoadherence of *P. falciparum* infected erythrocytes (iRBC) to several binding receptors on host vascular endothelium. Among them, binding to ICAM-1 seems to be related to severe manifestations of the disease such as cerebral malaria. The binding site for iRBC has been mapped to the BED-side of the N-terminal immunoglobulin-like domain of ICAM-1, and the DE-loop appears to be critical for binding. To date (+)-EGCG is the unique small molecule anti-cytoadherence inhibitor probably mimicking the DE-loop of ICAM-1. Here we report the discovery of a tetrahydroisoquinoline derivative, a prototype of a novel class of cytoadherence inhibitors, and an analogue of the natural compound characterized by a synthetically accessible scaffold. Molecular modeling analysis of (+)-EGCG and its synthetic tetrahydroisoquinoline analogue rationalized their binding mode to PfEMP1, confirming their ability to mimic the DE-loop.

Received 18th October 2013
Accepted 6th December 2013

DOI: 10.1039/c3ra45933k

www.rsc.org/advances

Introduction

Malaria is a deadly disease killing millions of people worldwide.¹ The disease is caused by infection from parasites of the genus *Plasmodium*. Several *Plasmodium* species affect humankind, e.g. *P. falciparum*, *P. vivax*, *P. ovale*, *P. malariae*, and *P. knowlesi*. Among them, *P. falciparum* is the most dangerous parasite and infection by *P. falciparum* can be lethal. The symptoms of uncomplicated malaria are normally mild and mainly comprise fever and headache. However, the symptoms

of severe malaria can rapidly develop from uncomplicated malaria resulting in coma and death. Among the manifestations of severe malaria, cerebral malaria is responsible for a significant proportion of mortality. Although the coma that characterizes cerebral malaria is likely to have multifactorial etiology, post-mortem analysis reveals a common feature, namely sequestration of infected red blood cells (iRBCs) in the microvasculature of the brain.^{2–4} Cytoadherence properties of iRBCs are mainly mediated by interaction of the parasite antigenic protein PfEMP1 with specific host receptors; mainly CD36, ICAM-1, or CSA (for placental malaria) located on the endothelial cell surface,^{5,6} although endothelial protein C receptor has recently been identified as an important ligand in cerebral malaria.⁷ PfEMP1 is expressed on the surface of the iRBCs and is encoded by around 60 divergent *var* genes.^{8–10} This surface antigenic protein is responsible for both adhesion and immune evasion.¹⁰ Although still debated,^{11,12} several studies highlighted a role of ICAM-1 binding for the development of cerebral malaria.^{3,13–15} ICAM-1 is expressed on the surface of leukocytes and endothelial cells and its expression is increased following inflammation.³ ICAM-1 is composed of five Ig-like domains.¹⁶ The binding site for PfEMP1 has been located in the N-terminal Ig-like domain and mainly involves 3 β -strands (named B, D, and E: the BED domain).¹⁷ On the other hand, PfEMP1 proteins are composed by modular domains: Duffy binding like (DBL) domains (classified into α - ζ), and cysteine rich interdomain regions (CIDR).^{18–20} Although a

^aEuropean Research Centre for Drug Discovery and Development (NatSynDrugs), Università degli Studi di Siena, via Aldo Moro 2, 53100 Siena, Italy. E-mail: campiani@unisi.it; Tel: +39 0577 234172

^bDipartimento di Biotecnologie, Chimica e Farmacia, Università degli Studi di Siena, via Aldo Moro 2, 53100 Siena, Italy

^cCentro Interuniversitario di Ricerche sulla Malaria (CIRM), University of Perugia, Perugia, Italy

^dDip. di Farmacia, University of Naples Federico II, Via D. Montesano 49, 80131 Naples, Italy

^eDepartment of Biochemistry, University of Cambridge, Cambridge, CB2 1GA, UK

^fDepartment of Biochemistry, University of Oxford, Oxford, OX1 3QU, UK

^gLiverpool School of Tropical Medicine, Pembroke Place, Liverpool L3 5QA, UK

† Electronic supplementary information (ESI) available: Figures S1–S5, Tables S1 and S2. See DOI: 10.1039/c3ra45933k

‡ Current address: Institute for Research in Molecular Medicine (INFORMM), University Sains Malaysia (USM), Health Campus, Kubang kerian, 16150 Kota Bharu, Kelantan, Malaysia.

crystallographic structure of an ICAM-1 binding PfEMP-1 has not been obtained yet, very recently a low resolution structure demonstrated a rigid and elongated arrangement of PfEMP1 domains.²¹ Moreover, in the same study it has been demonstrated that the binding of ICAM-1 to PfEMP1 is exclusively mediated through the DBL β domain.²¹ As shown by mutagenesis studies,²² several regions within this domain are probably involved in the interaction with ICAM-1, potentially within a relatively small region of the DBL β domain.²³

Cytoadhesion represents a novel and unexplored target process for drug development and due to its role in severe malaria, the discovery of small molecules able to interfere with interaction between PfEMP1 and its cellular receptor would represent useful adjunct therapeutic approaches for the treatment of severe malaria symptoms. However, the development of small molecule inhibitors is difficult and extremely challenging. Recently, the anti-adhesion properties of (+)-epigallocatechin gallate (EGCG, **1**, Fig. 1) have been reported.^{24,25} This molecule

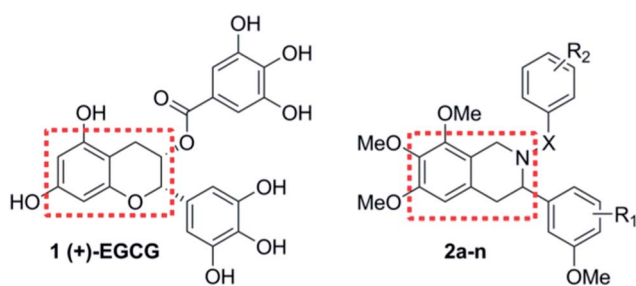


Fig. 1 Chemical structures of reference (**1**) and title (**2a–n**) compounds (R_1 , X , and R_2 are defined in Table 1).

Table 1 Inhibition of cytoadhesion (%) of compounds **2a–n** and reference compound **1** measured for the ItG strain under static conditions²⁵

Cpd	X	R_1	R_2	% Inhibition ^a	Fitness ^c	
					R	S
2a	COO	4-OMe	H	7	0.91	0.99
2b	COO	4-OMe	4-OMe	15	1.18	1.19
2c	COO	4-OMe	3,4-diOMe	13	1.16	1.15
2d	COO	5-OMe	H	16	1.16	1.20
2e	COO	5-OMe	4-OMe	20	1.17	1.14
2f	COO	5-OMe	3,4-diOMe	18	1.23	1.30
2g	CONH	4-OMe	3-OMe	12	1.27	0.92
2h	CONH	4-OMe	4-OMe	12	1.15	1.21
2i	CONH	5-OMe	3-OMe	11	1.05	1.09
2j	CONH	5-OMe	4-OMe	20	1.15	1.16
2k	CO	4-OMe	4-OMe	18	1.18	1.26
2l	CO	4-OMe	3,4,5-triOMe	21	1.20	1.27
2m	CO	5-OMe	4-OMe	13	1.03	1.19
2n	CO	5-OMe	3,4,5-triOMe	44	1.37	1.39
1	—	—	—	85 ^b	2.13	

^a Standard errors were all within 10% of the mean. The compounds have been dissolved in DMSO (8% DMSO final concentration in binding buffer). ^b Data from ref. 25. ^c Fitness is a score that represents how well the matching pharmacophore site of compounds (acceptors, donor, hydrophobic, etc.) align to those of the hypothesis.²⁷

was discovered through a virtual screening approach and it was hypothesized (although not proved) to mimic the structural features of the DE-loop of ICAM-1 BED-domain.²⁴ Its enantiomer (–)-EGCG was also tested and proved to be almost equally potent indicating a low degree of stereoselective interaction. Even considering recent progresses,²⁶ the synthesis of this natural compound is still a challenge. Moreover, the presence of two chiral centres, and the low stability of this heterocyclic system, could prevent the implementation of a medicinal chemistry approach aimed at discovering optimized inhibitors. Here we report the conversion of the epigallocatechin scaffold of EGCG into a tetrahydroisoquinoline system and the synthesis of a small library of derivatives (Fig. 1 and Table 1, **2a–n**) bearing different decoration patterns at the aromatic rings. In analogy to EGCG, also in this case the compounds were designed to target the DE-loop of ICAM-1 BED-domain. From these studies, we identified a suitable hit compound for further development and investigated its potential binding mode to PfEMP1 through molecular modeling studies. The isoquinoline **2n** is the first inhibitor of cytoadhesion, easily accessible and designed to interfere with the protein–protein interaction between ICAM-1 and PfEMP1.

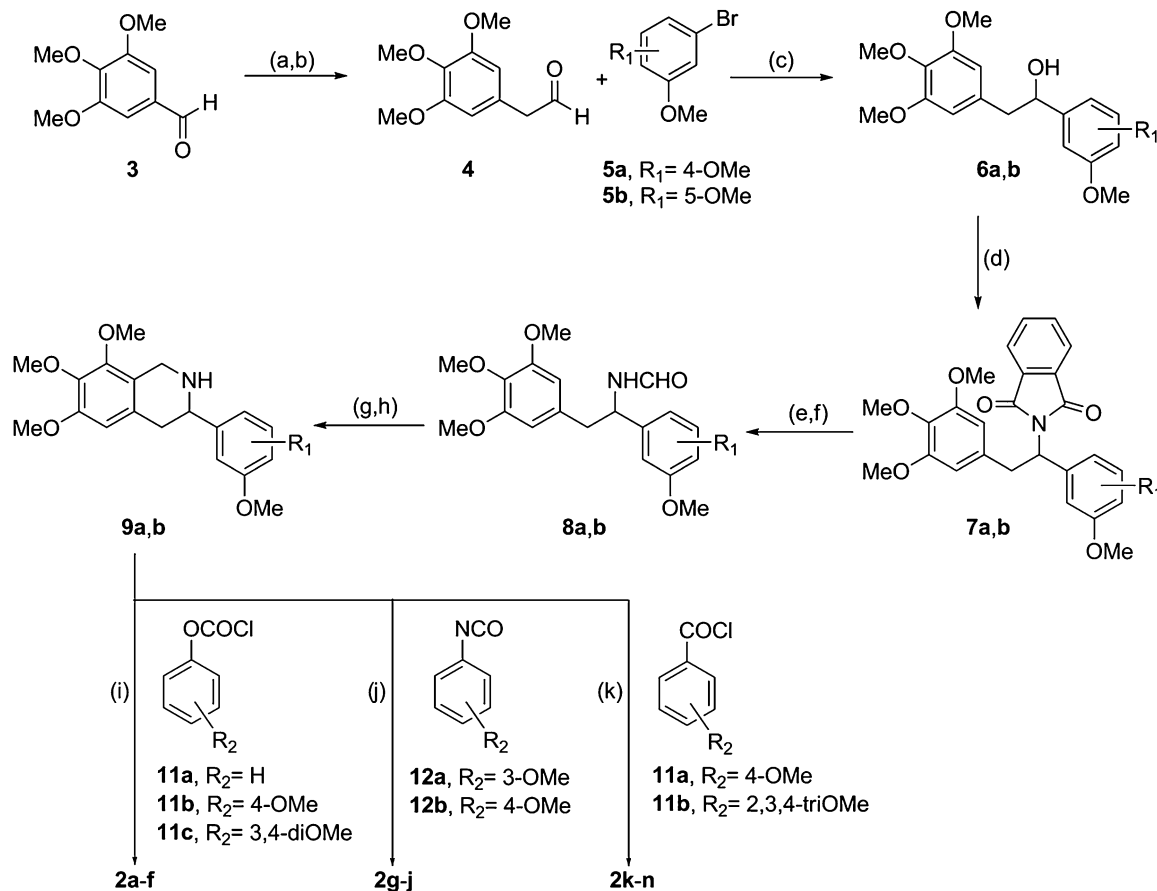
Chemistry

The synthesis of compounds **2a–n** is described in Scheme 1. Accordingly, aldehyde **3** was homologated to **4** through a two-step procedure. Firstly, the aldehyde group was converted into the corresponding vinyl ether through the Wittig reaction protocol; secondly, cleavage of the ether was accomplished under acidic conditions to afford **4**. The aldehyde was then reacted with the Grignard reagent obtained by treatment of bromides **5a,b** with Mg turnings. Mitsunobu reaction of the corresponding carbinols **6a,b** afforded phthalimides **7a,b**. The subsequent synthetic steps involved hydrazinolysis of the phthalimido group to release the free amines which were immediately treated with ethyl formate to afford formamides **8a,b**. Treatment of these latter compounds with POCl₃ afforded the corresponding dihydroisoquinolines, which were converted into **9a,b** through reduction of the imine double bond using sodium borohydride in methanol. The tetrahydroisoquinoline core of **9a,b** was further decorated by introducing appropriate methoxy-substituted aromatic rings linked to the heterocyclic nitrogen through different tethers.

Reaction of **9a,b** with chloroformates **11a,b**, isocyanates **12a,b**, and acyl chlorides **13a,b**, afforded the corresponding carbamates **2a–f**, ureas **2g–j**, and amides **2k–n**, respectively.

Results and discussion

The biological investigation of the library was accomplished as previously described using recombinant ICAM-1-Fc protein as the cytoadhesion target.^{24,25} The screening was performed using the ICAM-1 binding parasite strain ItG, which is a strong ICAM-1 binder.²⁵ Results are reported in Table 1. From the screening, compound **2n** resulted the best inhibitor of cytoadhesion with an inhibition potency (44% at 50 μ M) lower than the natural



Scheme 1 Synthetic procedure for the preparation of compounds **2a–n**; *Reagents and conditions*: (a) $\text{PPh}_3\text{CH}_2\text{OMeCl}$, NaHMDS, THF, from 0 °C to 25 °C, 6 h, 90%; (b) 4 N HCl, acetone, 25 °C, 3–4 h, 100%; (c) (i) **5a,b**, Mg, I_2 , THF, reflux, 1 h; (ii) **4**, THF, reflux, 10 h, 47–50%; (d) phthalimide, PPh_3 , DIAD, THF, from 0 °C to 25 °C, 10 h, 58–61%; (e) hydrazine hydrate, EtOH, reflux, 8 h, 55–60%; (f) ethylformate, reflux, 12 h, 56–62%; (g) POCl_3 , toluene, 90 °C, 3 h, 94–98%; (h) NaBH_4 , MeOH, from 0 °C to 25 °C, 1 h, 83–89%; (i) TEA, THF, 55 °C, 10 h 33–49%; (j) THF, 50 °C, 6 h, 45–51%; (k) TEA, DCM, from 0 °C to 25 °C, 6 h, 19–25%.

compound (+)-EGCG (85% at 50 μM) but still showing significant inhibition and being much more chemically accessible. The best compound of the series **2n** was also evaluated to investigate its effects on cell viability *in vitro*. Acute toxicity assay was performed against murine fibroblast cell line NIH3T3. Regrettably, the hit **2n** resulted endowed with an $\text{IC}_{50} = 72 \mu\text{M}$ on NIH3T3, which is almost comparable with its cytoadhesion inhibitory activity.

In order to understand the structural features responsible for the ability of compound **2n** to mimic the ICAM-1 DE-loop and to inhibit binding to PfEMP1, we undertook an in depth molecular modeling investigation. The *in silico* analysis was performed using the crystal structure of ICAM-1 (PDB ID: 1IAM) and a homology model of the DBL β domain since it has recently been demonstrated that the binding of ICAM-1 to PfEMP1 is exclusively mediated through this domain.²¹ In order to build the DBL β domain the information relative to the sequence to be modeled was extracted from a full length sequence of PfEMP1 IT4VAR13 (UniprotKB ID: A3R6S0; 3277AA) according to the recently published model.²¹ The selected domain was built applying a multiple template-based homology modeling approach successfully employed previously by means of

MODELLER package (details concerning the generation of the model are reported in the Experimental section, while the homology model analysis is provided in Fig. S1†).²⁸ It is worthy of note that two parallel protein refinement protocols have been applied and their outcomes compared. In the first procedure, after structure optimization by using MacroModel (MM), the DBL β domain homology model was submitted to Protein Preparation Wizard (PPW) (Method-1 MM-PPW). The second procedure envisaged the use of PPW in the first step of the homology model optimization procedure, with the MM minimization performed after a first run of PPW (Method-2 PPW-MM). Since no substantial changes were found between the two DBL β domain homology models, for convenience's sake only the output obtained with the first methodology is described in the Main Text, while the output obtained by using the second methodology is provided in ESI† together with the comparison of the two pharmacophores. The sequence concerning the ICAM-1^{D1D2} interacting domain was extracted from the crystal structure of this protein available from Protein Data Bank (PDB ID: 1IAM).²¹ The complex between the modeled DBL β domain and ICAM-1^{D1D2} was built by HADDOCK (High Ambiguity Driven protein–protein DOCKing) web server.²⁹ HADDOCK is an

information-driven flexible docking approach for the modeling of biomolecular complexes.³⁰

During the input steps, description of the interfaces that were involved in the protein–protein interaction was provided. The sequence of the DE-loop (L42–R49) of ICAM-1^{D1D2} was carefully chosen, while for the DBL β domain cavity a larger interface was selected according to the binding site prediction performed by SiteMap (Fig. S3[†]).³¹ The best complex obtained by means of HADDOCK web server was superimposed to the experimental SAXS (Small-Angle X-ray Scattering) data.²¹ The superposition between the SAXS data and the docked complex was performed by SUPCOMB.³² The complex was minimized taking into account constraint distances derived by experimental SAXS information using MacroModel.³³

This series of computational approaches based on the experimental model allowed us to increase the reliability of the homology modeling and protein–protein docking simulation. The obtained complex between the DBL β domain and ICAM-1^{D1D2} is depicted in Fig. 2, while the output of the second methodology is reported in Fig. S2.[†] The two different procedures conveyed in no substantial changes in the final complex between DBL β –ICAM^{D1D2} as demonstrated by their superimposition (Fig. S2[†]). As shown in Fig. 3, the DE-loop of ICAM^{D1D2} showed a strong pattern of interaction with the cleft of DBL β domain. In particular, a relevant number of residues located in the DE-loop are involved in polar contacts with residues of PfEMP1–DBL β domain (Fig. 3). The L42–R49 loop interacts with

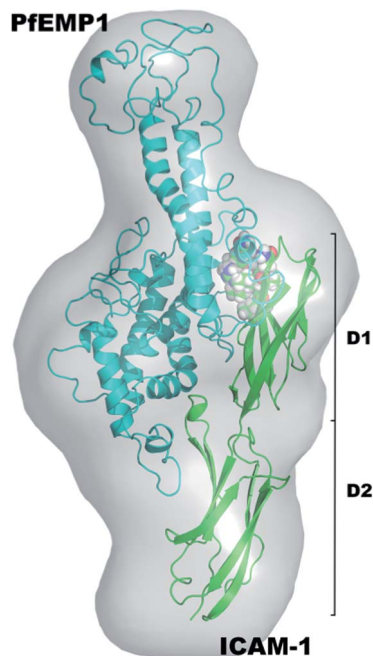


Fig. 2 Superposition between the DBL β –ICAM^{D1D2} (cyan and green cartoon, respectively) by HADDOCK web server and the shorter enveloped derived by experimental SAXS data.²¹ The DE-loop is represented by spheres. The picture was generated by PyMOL (PyMOL is an OPEN SOURCE program distributed under the “Python” license. The PyMOL Molecular Graphics System, v1.6-alpha; Schrodinger LLC: New York, 2013). Nonpolar hydrogens were omitted for the sake of clarity.

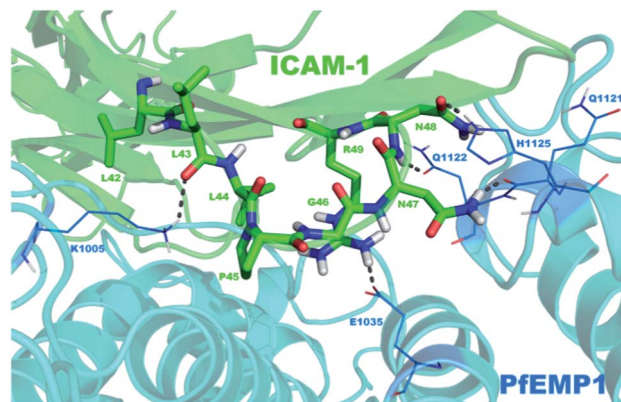


Fig. 3 Details of the DBL β –ICAM^{D1D2} complex (cyan and green cartoons, respectively). Key residues of the ICAM-1 docked into PfEMP1 DBL β binding domain are represented by green tubes and blue lines respectively. Hydrogen-bonds were reported as gray dotted lines. The numbering of PfEMP1 is referred to full length protein sequence (see Fig. S4 in the ESI[†] for further details). The picture was generated by PyMOL. Nonpolar hydrogens were omitted for the sake of clarity.

the DBL β domain by a series of polar contacts: the backbone carboxyl group of residue L43 produced a contact with K1005 belonging to PfEMP1; the side chain of R49 is involved in a hydrogen-bond with residue E1035 of PfEMP1, while the side chain of residue N47 produced a hydrogen-bond with the backbone of the residue Q1121 of PfEMP1. Moreover, the backbone NH and the side chain carbonyl group of N48 produced two hydrogen-bonds with Q1122 and H1125 belonging to the DBL β domain, respectively (the numbering of PfEMP1 residues above mentioned is referred to the full length protein sequence as shown in Fig. S4[†]). In the second step of our computational analysis, in order to evaluate the ability of compound **1** and **2n** to interact with the DBL β domain, mimicking the ICAM-1 DE-loop, a Structure-Based (SB) pharmacophore was developed, taking into account the interactions highlighted for the DE-loop reported in Fig. 3 and S2.[†] For this purpose the e-Pharmacophore application implemented in Maestro molecular modeling environment was used.^{33,34} This innovative method for generating SB pharmacophores combines pharmacophore perception with protein ligand energetic terms computed by the Glide XP (extra precision) scoring function (details of the SB pharmacophore generation are provided in the Experimental section).³⁵ Since the DBL β domain homology model was minimized using two different methods, both resulting DBL β –ICAM^{D1D2} complexes were used to generate a SB pharmacophore. The SB pharmacophore hypothesis (AADDHP) shown in Fig. 4 is referred to the Method-1 MM-PPW and consists of six features: two hydrogen-bond acceptors (A; represented by red vectors), two hydrogen-bond donors (D; represented by light blue vectors), one hydrophobic function (H; represented by a green sphere) and one positive ionizable centre (blue sphere). The SB pharmacophore obtained by using the complex deriving from DBL β domain minimized with Method-2 PPW-MM and the comparison between the two pharmacophore hypotheses are provided in ESI (Fig. S5[†]). The AADDHP SB pharmacophore was used to evaluate the fitness of

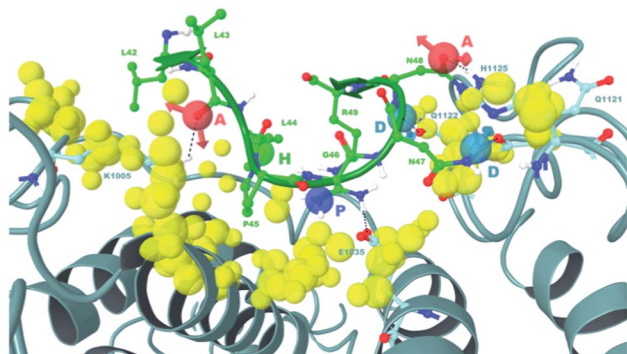


Fig. 4 AADDHP hypothesis generated by e-Pharmacophore. The DBL β domain is represented by turquoise ribbons and the key residues are reported as ball and stick, while the DE-loop is represented by green ribbons and ball and stick. The hydrogen-bonds between the key residues of DE-loop and the DBL β domain binding site are reported as gray dotted lines. Features are as follows: H-bond acceptors = A; red vector; hydrogen-bond donor = D; light blue vector; hydrophobic feature = H; green sphere; positive ionizable = P; blue sphere; excluded volumes = yellow spheres (The picture was generated by Maestro). Nonpolar hydrogens were omitted for the sake of clarity.

compounds reported in this study in order to rationalize their inhibitory activity. The outcome of these calculations are reported in Tables 1 and S1,[†] while the superposition between compounds **1** and **2n** and AADDHP hypothesis is shown in Fig. 5A and B, respectively (the superposition between all compounds and AADDHP hypothesis is reported in Table S2 of the ESI[†]). Both enantiomers of each compound were taken into consideration; no significant differences of fitness for each couple of enantiomers were observed.

Pharmacophore modeling studies were consistent with the different ability of the reference compound **1** and the synthetic analogues **2a–n** in disrupting the PfEMP1/ICAM-1 interaction. In particular, the absence of hydrogen-bond donor groups in the **2a–n** series is detrimental for the inhibition potency of these compounds compared to **1**. In fact, as reported in Fig. 5, compound **2n** is able to match only three features (two hydrogen-bond acceptor features and the hydrophobic function), while compound **1** matches four features when it is superposed onto the pharmacophore hypothesis AADDHP (two hydrogen-bond acceptor features and two hydrogen-bond donor features). In fact compound **1** and **2n** showed a fitness of 2.13 and 1.39 respectively. The same trend described for **2n** is observed for all the compounds reported in Table 1 of the Main Text (Table S2 of the ESI[†] depicts the superimposition between all the compounds and the AADDHP SB pharmacophore). All of them match the same three features of compound **2n**, although with different fitnesses. Concerning the fitness, the multiple substitutions of OMe in the aromatic ring at C3 of the tetrahydroisoquinolines **2f**, **2l** and **2n** results in a better matching of the pharmacophore features. Moreover, a OMe group at position 5' rather than 4' (R_1 substituent in Table 1), when coupled to a short linker (such as a carbonyl group) shows better results than longer linkers such as $-\text{COO}-$ or $-\text{CONH}-$. Finally, the lack of OMe groups at R_2 reduced dramatically the inhibitory

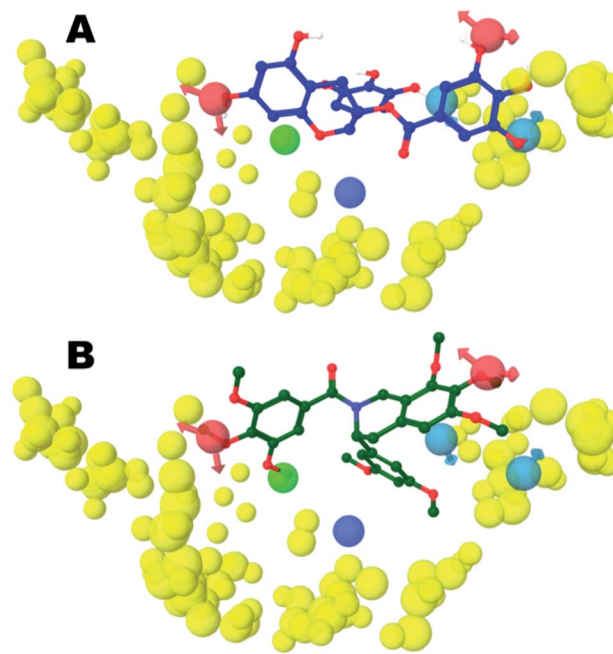


Fig. 5 (A) Superposition of SB pharmacophore and **1**. (B) Superposition of SB pharmacophore and **2n** *R*-enantiomer. Features are as follows: hydrogen-bond acceptor = red vector; hydrogen-bond donor = light blue vector; hydrophobic feature = green sphere; positive ionizable = blue sphere (The picture was generated by Maestro). Nonpolar hydrogens were omitted for the sake of clarity.

potency of the corresponding compound, especially in the 4-OMe sub-series (**2a**). Based on these considerations, the three-dimensional arrangement of **2n** assures the best fit onto the pharmacophore hypothesis AADDHP with respect to the other compounds in the series. In summary, the pharmacophore modeling studies are in good agreement with the experimental data displayed in Tables 1 and S1[†] and the computational methodology here reported was useful for highlighting the structural requirements necessary for the activity of the compounds.

Conclusions

Concluding, we successfully replaced the epigallocatechine core of (+)-EGCG with an appropriately decorated tetrahydroisoquinoline ring. Compounds bearing this latter molecular scaffold can be easily synthesized through straightforward synthetic procedures allowing rapid exploitation of the structure–activity relationships. The molecular modeling studies herein reported, based on a homology modeling approach for building the PfEMP1–DBL β domain coupled to protein–protein docking and experimental SAXS data²¹ allowed us to generate a reliable model of the DBL β –ICAM^{D1D2} complex. The subsequently developed SB pharmacophore, based on docking calculation, helped us to rationalize the inhibitory activity of both (+)-EGCG and **2n** against PfEMP1, highlighting that both compounds are able to mimic specific structural features of the ICAM-1 DE-loop. The information derived from the SB pharmacophore will guide the future hit-to-lead design of **2n**

analogues with improved anti-cytoadhesion properties. Furthermore, the cytotoxicity issue will be taken into account as additional parameter in the design of novel **2n** analogues.

Experimental

Chemistry

Unless otherwise specified, materials were purchased from commercial suppliers and used without further purification. Reaction progress was monitored by TLC using silica gel 60 F254 (0.040–0.063 mm) with detection by UV. Silica gel 60 (0.040–0.063 mm) was used for column chromatography. ^1H NMR spectra were recorded on a Varian 300 MHz spectrometer or a Bruker 400 MHz spectrometer by using the residual signal of the deuterated solvent as internal standard. Splitting patterns are described as singlet (s), doublet (d), triplet (t), quartet (q), and broad (br); the value of chemical shifts (δ) are given in ppm and coupling constants (J) in Hertz (Hz). ESI-MS spectra were performed by an Agilent 1100 Series LC/MSD spectrometer. ESI-MS spectra for exact mass determination were performed on a LTQ Orbitrap Thermo Fischer Scientific instrument. Melting points were determined in Pyrex capillary tubes using an Electrothermal 8103 apparatus and are uncorrected. Yields refer to purified products and are not optimized. All moisture-sensitive reactions were performed under argon atmosphere using oven-dried glassware and anhydrous solvents.

2-(3,4,5-Trimethoxyphenyl)acetaldehyde (4). To a suspension of chloro(methoxymethyl)triphenylphosphorane (3.8 g, 11.2 mmol) in dry THF (40 mL), 1 M solution of NaHMDS (10.7 mL, 10.7 mmol) was added slowly at 0 °C. After 30 min, a solution of 3,4,5-trimethoxy benzaldehyde **3** (2.0 g, 10.1 mmol) in dry THF (10 mL) was slowly added to the reaction mixture at 0 °C. Afterward, the reaction mixture was stirred at 25 °C for 6 h followed by quenching the reaction with saturated aqueous ammonium chloride. THF was evaporated *in vacuo* and the aqueous phase was extracted with ethyl acetate. The organic phase was washed with brine, dried over Na_2SO_4 and evaporated. The residue was purified by flash column chromatography using 10% ethyl acetate in hexane to afford 1,2,3-trimethoxy-5-(2-methoxyvinyl)benzene (2.05 g, 90%) as white solid and as a mixture of cis and trans isomers. ^1H NMR (400 MHz, acetone- d_6) δ 7.08 (d, $J = 12.9$ Hz, 1H), 6.82 (s, 2H), 6.52 (s, 2H), 6.11 (d, $J = 7.1$ Hz, 1H), 5.73 (d, $J = 12.9$ Hz, 1H), 5.08 (d, $J = 7.1$ Hz, 1H), 3.73 (s, 6H), 3.71 (s, 6H), 3.62 (s, 3H), 3.61 (s, 3H), 3.57 (s, 6H); ^{13}C NMR (75 MHz, CDCl_3) δ 153.6, 153.1, 148.8, 147.7, 136.6, 132.4, 131.8, 105.9, 105.7, 105.4, 102.5, 61.14, 61.09, 61.0, 56.8, 56.26, 56.21; MS (ESI) m/z 247 $[\text{M} + \text{Na}]^+$. To a solution of the above compound (1.0 g, 4.4 mmol) in acetone, 4 N HCl (5 mL) was added and the reaction mixture was stirred for 3–4 h at 25 °C. The reaction mixture was neutralised by adding 10% aqueous NaHCO_3 , acetone was evaporated and the aqueous phase was extracted with ethyl acetate. The organic phase was washed with brine, dried over Na_2SO_4 and evaporated to afford **4** (880 mg, 100%) as yellow low melting solid that was used in the next step without further purification.

1-(3,4-Dimethoxyphenyl)-2-(3,4,5-trimethoxyphenyl)ethanol (6a). A dry two necked round bottom flask, equipped with

dropping funnel and condenser under argon flow, was charged with freshly washed and dried magnesium turnings (268 mg, 11.6 mmol), a catalytic amount of iodine (5.0 mg, 0.02 mmol), and dry THF (10 mL). A solution of 3,4-dimethoxybromobenzene **5a** (2.5 g, 11.6 mmol) in dry THF (20 mL) was added dropwise, the reaction mixture was heated under reflux for 1 h after complete addition. A solution of aldehyde **4** (937 mg, 4.4 mmol) in dry THF (20 mL) was added to the reaction mixture at 70 °C and stirred for 10 h. The reaction mixture was cooled to 25 °C, and quenched by saturated aqueous ammonium chloride. THF was evaporated and the aqueous phase was extracted with ethyl acetate. The organic phase was washed with brine, dried over Na_2SO_4 and evaporated. The residue was purified by flash column chromatography using 25% ethyl acetate in hexane to afford **3a** (780 mg, 50%) as pale yellow solid. ^1H NMR (400 MHz, CDCl_3) δ 6.86–6.71 (m, 3H), 6.32 (s, 2H), 4.75 (dd, $J = 7.0$ Hz, 1H), 3.81 (s, 3H), 3.81 (s, 3H), 3.75 (s, 3H), 3.74 (s, 6H), 2.95–2.75 (m, 2H), 1.96 (bs, 1H); ^{13}C NMR (75 MHz, CDCl_3) δ 153.2, 149.0, 148.5, 136.8, 136.7, 134.0, 111.1, 109.4, 106.6, 75.1, 60.9, 56.2, 56.1, 56.0, 46.6; MS (ESI) m/z 371 $[\text{M} + \text{Na}]^+$; HRMS: calcd for $\text{C}_{19}\text{H}_{24}\text{NaO}_6$ $[\text{M} + \text{Na}]^+$ 371.1471, found 371.1473.

1-(3,5-Dimethoxyphenyl)-2-(3,4,5-trimethoxyphenyl)ethanol (6b). The title compound was prepared from **4** (250 mg, 1.1 mmol) and 3,5-dimethoxybromobenzene **5b** in a manner similar to that described for **6a**. The residue was purified by flash column chromatography using 35% ethyl acetate in hexane to afford **6b** (195 mg, 47%) as pale yellow solid. ^1H NMR (300 MHz, CDCl_3) δ 6.51 (m, 2H), 6.42–6.34 (m, 3H), 4.80 (dd, $J = 8.2, 4.8$ Hz, 1H), 3.81 (s, 6H), 3.81 (s, 3H), 3.77 (s, 3H), 3.77 (s, 3H), 3.02–2.80 (m, 2H), 1.81 (bs, 1H); ^{13}C NMR (75 MHz, CDCl_3) δ 46.5, 55.6, 56.3, 61.0, 75.4, 99.8, 104.0, 106.6, 133.8, 136.9, 146.6, 153.4, 161.1; MS (ESI) m/z 371 $[\text{M} + \text{Na}]^+$; HRMS: calcd for $\text{C}_{19}\text{H}_{24}\text{NaO}_6$ $[\text{M} + \text{Na}]^+$ 371.1471, found 371.1477.

2-(1-(3,4-Dimethoxyphenyl)-2-(3,4,5-trimethoxyphenyl)ethyl)-isoindoline-1,3-dione (7a). To a solution of **6a** (100 mg, 0.28 mmol), phthalimide (46.5 mg, 0.31 mmol) and triphenylphosphine (113 mg, 0.43 mmol) in dry THF (5 mL), diisopropyl azodicarboxylate (85 μL , 0.43 mmol) was added at 0 °C and the reaction mixture was stirred for 10 h at 25 °C. Afterward, the reaction mixture was concentrated and the residue was purified by flash column chromatography using 25% ethyl acetate in hexane to afford **13a** (80 mg, 58%) as pale yellow solid. ^1H NMR (400 MHz, CDCl_3) δ 7.71 (dd, $J = 5.5, 3.1$ Hz, 2H), 7.62 (dd, $J = 5.5, 3.0$ Hz, 2H), 7.22–7.12 (m, 2H), 6.82 (d, $J = 8.3$ Hz, 1H), 6.41 (s, 2H), 5.57 (dd, $J = 11.2, 5.7$ Hz, 1H), 3.94–3.86 (m, 1H), 3.89 (s, 3H), 3.84 (s, 3H), 3.72 (s, 3H), 3.70 (s, 6H), 3.37 (dd, $J = 14.0, 5.7$ Hz, 1H); ^{13}C NMR (75 MHz, CDCl_3) δ 168.6, 153.2, 149.1, 148.9, 136.7, 134.1, 138.8, 132.1, 131.8, 123.3, 120.8, 111.7, 111.1, 106.0, 61.0, 56.2, 56.1, 56.0, 55.9, 37.8, 22.1; MS (ESI) m/z 478 $[\text{M} + \text{H}]^+$, 500 $[\text{M} + \text{Na}]^+$; HRMS: calcd for $\text{C}_{27}\text{H}_{27}\text{NNaO}_7$ $[\text{M} + \text{Na}]^+$ 500.1685, found 500.1680.

2-(1-(3,5-Dimethoxyphenyl)-2-(3,4,5-trimethoxyphenyl)ethyl)-isoindoline-1,3-dione (7b). The title compound was prepared from **6b** (100 mg, 0.28 mmol) in a manner similar to that described for **7a**. The residue was purified by flash column chromatography using 28% ethyl acetate in hexane to afford **7b**

(84 mg, 61%) as yellow solid. ^1H NMR (400 MHz, CDCl_3) δ 7.66 (dd, $J = 5.4, 3.1$ Hz, 2H), 7.57 (dd, $J = 5.4, 3.1$ Hz, 2H), 6.71 (d, $J = 2.2$ Hz, 2H), 6.36 (s, 2H), 6.32 (t, $J = 2.2$ Hz, 1H), 5.50 (dd, $J = 11.3, 5.6$ Hz, 1H), 3.83 (dd, $J = 14.0, 11.4$ Hz, 1H), 3.72 (s, 6H), 3.67 (s, 3H), 3.65 (s, 6H), 3.32 (dd, $J = 14.0, 5.6$ Hz, 1H); ^{13}C NMR (75 MHz, $\text{DMSO}-d_6$) δ 168.6, 153.2, 149.2, 149.0, 136.6, 135.4, 134.4, 132.4, 131.6, 123.7, 120.4, 112.3, 112.2, 106.7, 60.6, 56.3, 56.2, 55.8, 37.6, 31.4; MS (ESI) m/z 500 $[\text{M} + \text{Na}]^+$; HRMS: calcd for $\text{C}_{27}\text{H}_{27}\text{NNaO}_7$ $[\text{M} + \text{Na}]^+$ 500.1685, found 500.1688.

***N*-(1-(3,4-Dimethoxyphenyl)-2-(3,4,5-trimethoxyphenyl)ethyl)-formamide (8a).** To a solution of **7a** (80 mg, 0.16 mmol) in ethanol (5.0 mL), hydrazine hydrate (40 μL , 0.08 mmol) was added and the reaction mixture was heated under reflux for 8 h. The reaction mixture was cooled to 25 $^\circ\text{C}$, filtered through filter paper and washed with ethanol. The combined organic phase was evaporated *in vacuo* to yield 50 mg (58%) of crude 1-(3,4-dimethoxyphenyl)-2-(3,4,5-trimethoxyphenyl)ethanamine as yellow sticky solid. The above crude amine was dissolved in the minimum amount of ethylformate and the resulting mixture was heated under reflux for 12 h. Subsequently, it was cooled to 25 $^\circ\text{C}$ and the ethylformate was removed by distillation. The crude residue was purified by flash column chromatography using chloroform to afford **8a** (55 mg, 56%) as white solid. ^1H NMR (300 MHz, CDCl_3) δ 8.18 (s, 1H), 6.89–6.73 (m, 2H), 6.70 (d, $J = 1.7$ Hz, 1H), 6.24 (d, $J = 3.4$ Hz, 2H), 5.85 (d, $J = 7.8$ Hz, 1H), 5.28 (dd, $J = 14.7, 7.2$ Hz, 1H), 3.85 (s, 3H), 3.82 (s, $J = 1.0$ Hz, 3H), 3.80 (s, 3H), 3.74 (s, 6H), 3.06 (t, $J = 6.5$ Hz, 2H) $^+$; ^{13}C NMR (75 MHz, CDCl_3) δ 207.1, 160.5, 153.2, 149.2, 148.7, 136.9, 133.7, 132.7, 118.7, 111.4, 110.5, 106.7, 106.5, 61.0, 56.3, 56.26, 56.20, 56.1, 53.0, 42.9, 31.1; MS (ESI) m/z 376 $[\text{M} + \text{H}]^+$ HRMS: calcd for $\text{C}_{20}\text{H}_{26}\text{NO}_6$ $[\text{M} + \text{H}]^+$ 376.1760, found 376.1760.

***N*-(1-(3,5-Dimethoxyphenyl)-2-(3,4,5-trimethoxyphenyl)ethyl)-formamide (8b).** The title compound was prepared from **7b** (150 mg, 0.43 mmol) in a manner similar to that described for **8a**. The residue was purified by flash column chromatography using 30% ethyl acetate and 0.1% TEA in hexane to afford **8b** (75 mg, 63%) as white solid. mp (hexane) 170–172 $^\circ\text{C}$; ^1H NMR (400 MHz, CDCl_3) δ 8.17 (s, 1H), 6.43–6.30 (m, 3H), 6.23 (d, $J = 3.4$ Hz, 2H), 5.79 (d, $J = 7.6$ Hz, 1H), 5.34–5.18 (m, 1H), 3.79 (s, 3H), 3.77 (s, 6H), 3.74 (s, 6H), 3.12–2.99 (m, 2H); MS (ESI) m/z 376 $[\text{M} + \text{H}]^+$, 398 $[\text{M} + \text{Na}]^+$; HRMS: calcd for $\text{C}_{20}\text{H}_{26}\text{NO}_6$ $[\text{M} + \text{H}]^+$ 376.1760, found 376.1755.

3-(3,4-Dimethoxyphenyl)-6,7,8-trimethoxy-1,2,3,4-tetrahydroisoquinoline (9a). To a solution of **8a** (50 mg, 0.13 mmol) in dry toluene (3.0 mL), phosphorus oxychloride (0.106 mL, 1.16 mmol) was added dropwise. The reaction mixture was stirred for 3 h at 90 $^\circ\text{C}$, then cooled to 0 $^\circ\text{C}$ and slowly quenched with 10% aqueous ammonia solution. Toluene was evaporated and the aqueous phase was extracted with ethyl acetate, the organic phase was washed with brine, dried over Na_2SO_4 and evaporated *in vacuo* to get 42 mg (98%) of 3-(3,4-dimethoxyphenyl)-6,7,8-trimethoxy-3,4-dihydroisoquinoline. To a solution of the crude dihydroisoquinoline (50 mg, 0.14 mmol) dissolved in methanol (5.0 mL), sodium borohydride (55 mg, 1.4 mmol) was added portion wise at 0 $^\circ\text{C}$. The reaction mixture was stirred for next 1 h at 25 $^\circ\text{C}$, and then was quenched by adding water. Methanol was evaporated *in vacuo* and the aqueous phase was extracted with

ethyl acetate. The organic phase was washed with brine, dried over Na_2SO_4 and evaporated *in vacuo*. The residue was purified by flash column chromatography using 1% methanol and 0.1% TEA in chloroform to afford **9a** (45 mg, 90%) as pale yellow solid. ^1H NMR (400 MHz, CDCl_3) δ 6.99 (d, $J = 1.9$ Hz, 1H), 6.92 (dd, $J = 8.2, 1.9$ Hz, 1H), 6.83 (dd, $J = 8.2, 3.2$ Hz, 1H), 6.39 (s, 1H), 4.22 (d, $J = 15.8$ Hz, 1H), 4.00 (d, $J = 15.9$ Hz, 1H), 3.87 (s, 3H), 3.86 (dd, $J = 5.6, 2.2$ Hz, 1H), 3.86 (s, 6H), 3.83 (s, 3H), 3.80 (s, 3H), 3.01–2.72 (m, 2H), 1.89 (bs, 1H); ^{13}C NMR (75 MHz, CDCl_3) δ 152.2, 150.3, 149.4, 148.5, 140.3, 137.1, 130.6, 121.1, 118.9, 111.3, 109.8, 107.7, 61.1, 60.7, 58.4, 56.2, 56.16, 56.13, 44.6, 38.0; MS (ESI) m/z 360 $[\text{M} + \text{H}]^+$, 382 $[\text{M} + \text{Na}]^+$; HRMS: calcd for $\text{C}_{20}\text{H}_{26}\text{NO}_5$ $[\text{M} + \text{H}]^+$ 360.1811, found 360.1817.

3-(3,5-Dimethoxyphenyl)-6,7,8-trimethoxy-1,2,3,4-tetrahydroisoquinoline (9b). The title compound was prepared from **8b** (105 mg, 0.29 mmol) in a manner similar to that described for **9a**. The residue was purified by flash column chromatography using 30% ethyl acetate in hexane to afford **9b** (89 mg, 83%) as off white solid. ^1H NMR (400 MHz, CDCl_3) δ 6.58 (d, $J = 2.2$ Hz, 2H), 6.43–6.33 (m, 2H), 4.22 (d, $J = 15.8$ Hz, 1H), 3.99 (d, $J = 15.8$ Hz, 1H), 3.87 (s, 3H), 3.83 (s, 3H), 3.80 (s, 3H), 3.77 (s, 6H), 2.94–2.77 (m, 2H), 1.89 (s, 2H); MS (ESI) m/z 360 $[\text{M} + \text{H}]^+$; HRMS: calcd for $\text{C}_{20}\text{H}_{26}\text{NO}_5$ $[\text{M} + \text{H}]^+$ 360.1811, found 360.1812.

***N*-(Phenoxycarbonyl)-3-(3,4-Dimethoxyphenyl)-6,7,8-trimethoxy-1,2,3,4-tetrahydroisoquinoline (2a).** To a solution of **9a** (125 mg, 0.34 mmol) and TEA (0.145 mL, 1.0 mmol) in dry THF (5.0 mL), was added phenyl chloroformate **11a** (87 μL , 0.69 mmol) and the reaction mixture was stirred at 55 $^\circ\text{C}$ for 10 h. The reaction was quenched by adding 10% aqueous NaHCO_3 , THF was removed and the aqueous phase was extracted with ethyl acetate. The organic phase was washed with brine, dried over Na_2SO_4 and evaporated. The residue was purified by flash chromatography using 25% ethyl acetate in hexane to afford **2a** (68 mg, 41%) as white solid. mp (hexane) 64–66 $^\circ\text{C}$; ^1H NMR (400 MHz, CDCl_3) δ 7.33 (s, 2H), 7.28–6.96 (m, 3H), 6.72 (s, 3H), 6.50 (s, 1H), 5.67 (bs, 1H), 4.99 (bs, 1H), 4.18 (bs, 1H), 3.95–3.77 (m, 12H), 3.73 (s, 3H), 3.37 (d, $J = 14.8$ Hz, 1H), 3.08 (d, $J = 15.7$ Hz, 1H); ^{13}C NMR (75 MHz, CDCl_3) δ 154.5, 152.8, 151.6, 150.0, 149.0, 148.4, 140.5, 129.4, 128.8, 125.5, 121.9, 119.3, 111.1, 111.0, 107.3, 61.1, 60.9, 56.2, 56.0, 55.9, 39.3; MS (ESI) m/z 480 $[\text{M} + \text{H}]^+$; HRMS: calcd for $\text{C}_{27}\text{H}_{30}\text{NO}_7$ $[\text{M} + \text{H}]^+$ 480.2022, found 480.2030; elemental calcd C, 67.63; H, 6.10; N, 2.92 for $\text{C}_{27}\text{H}_{29}\text{NO}_7$; found C, 67.92; H, 5.91; N, 2.57%.

***N*-(4-Methoxyphenoxycarbonyl)-3-(3,4-Dimethoxyphenyl)-6,7,8-trimethoxy-1,2,3,4-tetrahydroisoquinoline (2b).** The title compound was prepared from **9a** (125 mg, 0.34 mmol) and 4-methoxyphenyl chloroformate **11b** (0.103 mL, 0.68 mmol) in a manner similar to that described for **2a**. The residue was purified by flash chromatography using 30% ethyl acetate in hexane to afford **2b** (87 mg, 49%) as pale yellow solid. mp (hexane) 60–62 $^\circ\text{C}$; ^1H NMR (400 MHz, CDCl_3) δ 7.00 (s, 2H), 6.84 (d, $J = 8.3$ Hz, 2H), 6.71 (s, 3H), 6.50 (s, 1H), 5.66 (s, 1H), 4.97 (s, 1H), 4.17 (s, 1H), 3.85 (s, 3H), 3.83 (s, 6H), 3.81 (s, $J = 7.7$ Hz, 3H), 3.77 (s, $J = 6.3$ Hz, 3H), 3.72 (s, 3H), 3.36 (dd, $J = 15.9, 6.0$ Hz, 1H), 3.07 (d, $J = 15.9$ Hz, 1H); ^{13}C NMR (75 MHz, CDCl_3) δ 157.1, 154.9, 152.8, 150.0, 149, 148.3, 145.1, 140.5, 128.8, 122.7, 119.2, 119.1, 114.5, 111.0, 107.3, 61.1, 60.9, 56.2, 56.0, 55.9, 55.8, 39.2, 39.1;

MS (ESI) m/z 532 $[M + Na]^+$; HRMS: calcd for $C_{28}H_{31}NNaO_8$ $[M + Na]^+$ 532.1947, found 532.1940; elemental calcd C, 66.00; H, 6.13; N, 2.75 for $C_{28}H_{31}NO_8$; found C, 65.74; H, 6.45; N, 2.89%.

N-(3,4-Dimethoxyphenoxycarbonyl)-3-(3,4-Dimethoxyphenyl)-6,7,8-trimethoxy-1,2,3,4-tetrahydroisoquinoline (2c). The title compound was prepared from **9a** (125 mg, 0.34 mmol) and 3,4-dimethoxyphenyl chloroformate **11c** (151 mg, 0.69 mmol) in a manner similar to that described for **2a**. The residue was purified by flash chromatography using 50% ethyl acetate in hexane to afford **2c** (63 mg, 33%) of as off white solid. mp (hexane) 67–69 °C; 1H NMR (400 MHz, $CDCl_3$) δ 6.84–6.76 (m, 1H), 6.71 (s, 3H), 6.62 (bs, 2H), 6.49 (s, 1H), 5.64 (bs, 1H), 4.95 (bs, 1H), 4.17 (bs, 1H), 3.85 (s, 3H), 3.83 (s, 6H), 3.83 (s, 6H), 3.80 (s, 3H), 3.72 (s, 3H), 3.36 (dd, $J = 16.0$, 6.1 Hz, 1H), 3.07 (d, $J = 15.9$ Hz, 1H); ^{13}C NMR (75 MHz, $CDCl_3$) δ 154.8, 152.8, 150.0, 149.4, 149, 140.4, 146.8, 145.3, 140.5, 133.9, 128.8, 119.3, 119.2, 113.3, 111.3, 111.1, 110.6, 107.3, 106.3, 61.1, 60.9, 56.4, 56.2, 56.1, 56.0, 55.9, 39.3; MS (ESI) m/z 540 $[M + H]^+$; HRMS: calcd for $C_{29}H_{34}NO_9$ $[M + H]^+$ 540.2234, found 540.2234; elemental calcd C, 64.55; H, 6.16; N, 2.60 for $C_{29}H_{33}NO_9$; found C, 64.50; H, 5.92; N, 2.96%.

N-(Phenoxycarbonyl)-3-(3,5-Dimethoxyphenyl)-6,7,8-trimethoxy-1,2,3,4-tetrahydroisoquinoline (2d). The title compound was prepared from **9b** (125 mg, 0.34 mmol) and phenyl chloroformate **11a** (87 μ L, 0.69 mmol) in a manner similar to that described for **2a**. The residue was purified by flash chromatography using 25% ethyl acetate in hexane to afford **2d** (76 mg, 45%) as off white solid. mp (hexane) 132–134 °C; 1H NMR (400 MHz, $CDCl_3$) δ 7.39–7.28 (m, 2H), 7.22–6.94 (m, 3H), 6.48 (s, 1H), 6.36 (d, $J = 1.7$ Hz, 2H), 6.30 (d, $J = 2.0$ Hz, 1H), 5.61 (bs, 1H), 5.00 (bs, 1H), 4.24 (d, $J = 15.7$ Hz, 1H), 3.85 (d, $J = 12.9$ Hz, 9H), 3.69 (s, 6H), 3.34 (dd, $J = 16.0$, 6.1 Hz, 1H), 3.08 (d, $J = 15.9$ Hz, 1H); ^{13}C NMR (75 MHz, $CDCl_3$) δ 161.0, 154.5, 152.8, 151.6, 149.9, 138.7, 129.4, 128.7, 125.5, 121.9, 107.3, 105.2, 99.1, 61.1, 60.9, 56.2, 55.4, 39.4, 32.8, 32.6; MS (ESI) m/z 502 $[M + Na]^+$; HRMS: calcd for $C_{27}H_{29}NNaO_7$ $[M + Na]^+$ 502.1842, found 502.1840; elemental calcd C, 67.63; H, 6.10; N, 2.92 for $C_{27}H_{29}NO_7$; found C, 67.75; H, 6.31; N, 2.63%.

N-(4-Methoxyphenoxycarbonyl)-3-(3,5-Dimethoxyphenyl)-6,7,8-trimethoxy-1,2,3,4-tetrahydroisoquinoline (2e). The title compound was prepared from **9b** (125 mg, 0.34 mmol) and 4-methoxyphenyl chloroformate **11b** (0.103 mL, 0.69 mmol) in a manner similar to that described for **2a**. The residue was purified by flash chromatography using 35% ethyl acetate in hexane to afford **2e** (62 mg, 35%) as white solid. mp (hexane) 58–60 °C; 1H NMR (400 MHz, $CDCl_3$) δ 6.97 (bs, 2H), 6.80 (s, 2H), 6.43 (s, 1H), 6.31 (s, 2H), 6.25 (s, 1H), 5.56 (bs, 1H), 4.95 (bs, 1H), 4.20 (s, 1H), 3.80 (d, $J = 14.3$ Hz, 9H), 3.71 (s, 3H), 3.63 (s, 6H), 3.28 (d, $J = 11.2$ Hz, 1H), 3.02 (d, $J = 15.2$ Hz, 1H); ^{13}C NMR (75 MHz, $CDCl_3$) δ 161.0, 157.1, 154.9, 152.8, 150, 145.1, 140.5, 128.7, 122.7, 114.5, 107.3, 105.3, 99.0, 61.1, 60.9, 56.2, 55.8, 55.4, 39.4, 37.1; MS (ESI) m/z 532 $[M + Na]^+$; HRMS: calcd for $C_{28}H_{31}NNaO_8$ $[M + Na]^+$ 532.1947, found 532.1946; elemental calcd C, 66.00; H, 6.13; N, 2.75 for $C_{28}H_{31}NO_8$; found C, 65.73; H, 5.78; N, 2.70%.

N-(3,4-Dimethoxyphenoxycarbonyl)-3-(3,5-Dimethoxyphenyl)-6,7,8-trimethoxy-1,2,3,4-tetrahydroisoquinoline (2f). The title compound was prepared from **9b** (125 mg, 0.34 mmol) and 3,4-

dimethoxyphenyl chloroformate **11c** (151 mg, 0.69 mmol) in a manner similar to that described for **2a**. The residue was purified by flash chromatography using 50% ethyl acetate in hexane to afford **2f** (80 mg, 44%) as pale yellow solid. mp (hexane) 57–59 °C; 1H NMR (400 MHz, $CDCl_3$) δ 6.88–6.78 (m, 1H), 6.67 (bs, 2H), 6.50 (s, 1H), 6.39 (d, $J = 2.1$ Hz, 2H), 6.32 (t, $J = 2.2$ Hz, 1H), 5.62 (bs, 1H), 5.00 (bs, 1H), 4.29 (bs, 1H), 3.89 (s, 3H), 3.85 (s, 12H), 3.71 (s, 6H), 3.36 (dd, $J = 16.0$, 6.1 Hz, 1H), 3.10 (d, $J = 15.9$ Hz, 1H); ^{13}C NMR (300 MHz, $CDCl_3$) δ 159.7, 153.6, 151.6, 148.7, 148.2, 145.5, 144.0, 139.3, 127.5, 112.0, 111.2, 110.1, 106.0, 105.0, 104.1, 97.7, 75.6, 59.9, 59.7, 55.1, 55.0, 54.9, 54.2, 38.2; MS (ESI) m/z 540 $[M + H]^+$, 562 $[M + Na]^+$; HRMS: calcd for $C_{29}H_{34}NO_9$ $[M + H]^+$ 540.2234, found 540.2230; elemental calcd C, 64.55; H, 6.16; N, 2.60 for $C_{29}H_{33}NO_9$; found C, 64.48; H, 6.24; N, 2.32%.

N-(3-Methoxyphenylaminocarbonyl)-3-(3,4-Dimethoxyphenyl)-6,7,8-trimethoxy-1,2,3,4-tetrahydroisoquinoline (2g). To a solution of **9a** (125 mg, 0.34 mmol) and TEA (0.145 mL, 1.0 mmol) in dry THF (5.0 mL), was added 3-methoxyphenyl isocyanate **12a** (45 μ L, 0.34 mmol) and the reaction mixture was stirred at 55 °C for 6 h. The reaction mixture was quenched by adding water, THF was removed and the aqueous phase was extracted with ethyl acetate. The organic phase was washed with 1 N HCl, brine, dried over Na_2SO_4 and evaporated *in vacuo*. The residue was purified by flash chromatography using 30% ethyl acetate in hexane to afford **2g** (85 mg, 48%) as off white solid. mp (hexane) 101–103 °C; 1H NMR (300 MHz, $CDCl_3$) δ 7.15–7.00 (m, 2H), 6.78 (d, $J = 0.9$ Hz, 2H), 6.62 (dd, $J = 8.0$, 1.2 Hz, 1H), 6.59–6.50 (m, 2H), 6.43 (s, 1H), 6.40 (s, 1H), 5.27–5.22 (m, 1H), 4.74–4.58 (m, 2H), 3.92 (s, 3H), 3.85 (s, 3H), 3.85 (s, 3H), 3.81 (s, 3H), 3.76 (s, 3H), 3.70 (s, 3H), 3.30 (dd, $J = 15.2$, 5.8 Hz, 1H), 2.93 (dd, $J = 15.2$, 4.1 Hz, 1H); ^{13}C NMR (75 MHz, $CDCl_3$) δ 160.3, 155.6, 152.9, 149.9, 149.5, 148.8, 140.8, 140.5, 134.4, 129.8, 129.6, 120.4, 118.6, 111.9, 111.3, 109.6, 109.0, 107.4, 105.4, 61.4, 61.2, 56.3, 56.0, 55.9, 55.4, 55.1, 39.0, 36.7; MS (ESI) m/z 509 $[M + H]^+$, 531 $[M + Na]^+$; HRMS: calcd for $C_{28}H_{33}N_2O_7$ $[M + H]^+$ 509.2288, found 509.2285; elemental calcd C, 66.13; H, 6.34; N, 5.51 for $C_{28}H_{32}N_2O_7$; found C, 66.30; H, 6.00; N, 5.27%.

N-(4-Methoxyphenylaminocarbonyl)-3-(3,4-Dimethoxyphenyl)-6,7,8-trimethoxy-1,2,3,4-tetrahydroisoquinoline (2h). The title compound was prepared from **9a** (125 mg, 0.34 mmol) and 4-methoxyphenyl isocyanate **12b** (45 μ L, 0.34 mmol) in a manner similar to that described for **2g**. The residue was purified by flash chromatography using 30% ethyl acetate in hexane to afford **2h** (91 mg, 51%) as off white solid. mp (hexane) 73–75 °C; 1H NMR (300 MHz, $CDCl_3$) δ 7.10 (dd, $J = 9.0$, 2.9 Hz, 2H), 6.82–6.71 (m, 4H), 6.59 (s, 1H), 6.43 (s, 1H), 6.27 (s, 1H), 5.32–5.23 (m, 1H), 4.71 (d, $J = 12.7$ Hz, 1H), 4.56 (d, $J = 15.4$ Hz, 1H), 3.89 (s, 3H), 3.83 (s, 6H), 3.79 (s, 3H), 3.72 (s, 3H), 3.69 (s, 3H), 3.29 (d, $J = 15.2$ Hz, 1H), 2.93 (d, $J = 15.2$ Hz, 1H); ^{13}C NMR (75 MHz, $CDCl_3$) δ 156.1, 155.9, 152.9, 149.9, 149.4, 148.7, 140.7, 134.5, 132.2, 129.8, 122.2, 120.4, 118.6, 114.2, 111.3, 109.6, 107.3, 61.4, 61.1, 56.2, 56.0, 55.9, 55.6, 54.7, 39.0, 36.5; MS (ESI) m/z 509 $[M + H]^+$; HRMS: calcd for $C_{28}H_{33}N_2O_7$ $[M + H]^+$ 509.2288, found 509.2231; elemental calcd C, 66.13; H, 6.34; N, 5.51 for $C_{28}H_{32}N_2O_7$; found C, 66.01; H, 6.02; N, 5.70%.

N-(3-Methoxyphenylaminocarbonyl)-3-(3,5-Dimethoxyphenyl)-6,7,8-trimethoxy-1,2,3,4-tetrahydroisoquinoline (2i). The title compound was prepared from **9b** (125 mg, 0.34 mmol) and **12a** in

a manner similar to that described for **2g**. The residue was purified by flash chromatography using 35% ethyl acetate in hexane to afford **20a** (80 mg, 45%) as white solid. mp (hexane) 68–70 °C; $^1\text{H NMR}$ (300 MHz, CDCl_3) δ 7.15–7.03 (m, 2H), 6.65 (dd, $J = 8.1, 1.9$ Hz, 1H), 6.54 (dd, $J = 7.0, 1.2$ Hz, 1H), 6.44 (s, 1H), 6.38 (s, 1H), 6.33 (s, 2H), 5.18 (t, $J = 5.2$ Hz, 1H), 4.79 (d, $J = 15.3$ Hz, 1H), 4.59 (d, $J = 15.3$ Hz, 1H), 3.92 (s, 3H), 3.85 (s, 3H), 3.81 (s, 3H), 3.77 (s, 3H), 3.70 (s, 6H), 3.28 (dd, $J = 15.2, 5.8$ Hz, 1H), 2.96 (dd, $J = 15.3, 4.7$ Hz, 1H); $^{13}\text{C NMR}$ (75 MHz, CDCl_3) δ 161.4, 160.3, 155.5, 152.9, 149.9, 144.6, 140.8, 140.5, 129.7, 129.6, 120.4, 111.9, 109.1, 107.3, 105.4, 104.5, 99.7, 61.4, 61.2, 56.3, 55.6, 55.5, 55.4, 39.0, 36.6; MS (ESI) m/z 509 $[\text{M} + \text{H}]^+$; HRMS: calcd for $\text{C}_{28}\text{H}_{33}\text{N}_2\text{O}_7$ $[\text{M} + \text{H}]^+$ 509.2288, found 509.2233; elemental calcd C, 66.13; H, 6.34; N, 5.51 for $\text{C}_{28}\text{H}_{32}\text{N}_2\text{O}_7$; found C, 66.40; H, 6.42; N, 5.85%.

N-(4-Methoxyphenylaminocarbonyl)-3-(3,5-Dimethoxyphenyl)-6,7,8-trimethoxy-1,2,3,4-tetrahydroisoquinoline (2j). The title compound was prepared from **9b** (125 mg, 0.34 mmol) and **12b** (45 μL , 0.34 mmol) in a manner similar to that described for **2g**. The residue was purified by flash chromatography using 30% ethyl acetate in hexane to afford **20b** (90 mg, 51%) as white solid. mp (hexane) 72–74 °C; $^1\text{H NMR}$ (400 MHz, CDCl_3) δ 7.11 (d, $J = 8.9$ Hz, 2H), 6.76 (d, $J = 8.9$ Hz, 2H), 6.43 (s, 1H), 6.32 (s, 3H), 6.21 (s, 1H), 5.19 (t, $J = 5.1$ Hz, 1H), 4.79 (d, $J = 15.3$ Hz, 1H), 4.52 (d, $J = 15.3$ Hz, 1H), 3.90 (s, 3H), 3.83 (s, 3H), 3.79 (s, 3H), 3.73 (s, 3H), 3.68 (s, 6H), 3.25 (dd, $J = 15.2, 5.8$ Hz, 1H), 2.94 (dd, $J = 15.3, 4.7$ Hz, 1H); $^{13}\text{C NMR}$ (75 MHz, CDCl_3) δ 161.3, 156.0, 155.9, 152.9, 149.9, 144.7, 140.8, 132.3, 129.7, 122.3, 120.5, 114.2, 107.3, 104.5, 99.6, 61.4, 61.2, 56.3, 55.7, 55.5, 55.3, 39.0, 36.5; MS (ESI) m/z 509 $[\text{M} + \text{H}]^+$; HRMS: calcd for $\text{C}_{28}\text{H}_{33}\text{N}_2\text{O}_7$ $[\text{M} + \text{H}]^+$ 509.2288, found 509.2288; elemental calcd C, 66.13; H, 6.34; N, 5.51 for $\text{C}_{28}\text{H}_{32}\text{N}_2\text{O}_7$; found C, 66.46; H, 6.13; N, 5.81%.

N-(4-Methoxybenzoyl)-3-(3,4-Dimethoxyphenyl)-6,7,8-trimethoxy-1,2,3,4-tetrahydroisoquinoline (2k). To the solution of **9a** (125 mg, 0.34 mmol) and TEA (0.145 mL, 1.0 mmol) in 5 mL dry DCM, was added 4-methoxybenzoyl chloride **13a** (72 μL , 0.52 mmol) at 0 °C and the reaction mixture was stirred for 6 h at 25 °C. The reaction mixture was diluted with DCM and washed with 10% aqueous NaHCO_3 , brine, dried over Na_2SO_4 and evaporated *in vacuo*. The residue was purified by flash chromatography using 35% ethyl acetate in hexane to afford **2k** (91 mg, 24%) as pale yellow solid. mp (hexane) 64–66 °C; $^1\text{H NMR}$ (300 MHz, $\text{DMSO}-d_6$, 353 K) δ 7.39 (d, $J = 8.7$ Hz, 2H), 6.99 (d, $J = 8.7$ Hz, 2H), 6.83 (d, $J = 8.1$ Hz, 1H), 6.67 (d, $J = 8.8$ Hz, 3H), 5.47 (bs, 1H), 4.80 (d, $J = 16.9$ Hz, 1H), 3.98 (d, $J = 17.1$ Hz, 1H), 3.80 (s, 3H), 3.77 (s, 3H), 3.70 (s, 6H), 3.69 (s, 3H), 3.64 (s, 3H), 3.33–3.12 (m, 2H); $^{13}\text{C NMR}$ (75 MHz, CDCl_3) δ 160.9, 152.8, 149.4, 149.3, 148.4, 140.2, 132.8, 129.3, 129.0, 119.0, 114.5, 112.3, 110.7, 110.6, 108.4, 61.0, 61, 56.5, 56.0, 56.0, 55.9, 32.8; MS (ESI) m/z 494 $[\text{M} + \text{H}]^+$; HRMS: calcd for $\text{C}_{28}\text{H}_{32}\text{NO}_7$ $[\text{M} + \text{H}]^+$ 494.2179, found 494.2180; elemental calcd C, 68.14; H, 6.33; N, 2.84 for $\text{C}_{28}\text{H}_{31}\text{NO}_7$; found C, 67.76; H, 5.99; N, 2.63%.

N-(3,4,5-Trimethoxybenzoyl)-3-(3,4-Dimethoxyphenyl)-6,7,8-trimethoxy-1,2,3,4-tetrahydroisoquinoline (2l). The title compound was prepared from **9a** (125 mg, 0.34 mmol) and 3,4,5-trimethoxybenzoyl chloride **13b** (160 mg, 0.69 mmol) in a manner similar to that described for **2k**. The residue was

purified by flash chromatography using 70% ethyl acetate in hexane to afford **2l** (37 mg, 19%) as white solid. mp (hexane) 144–146 °C; $^1\text{H NMR}$ (300 MHz, $\text{DMSO}-d_6$, 353 K) δ 6.83 (d, $J = 8.1$ Hz, 1H), 6.72–6.63 (m, 5H), 5.37 (bs, 1H), 4.84 (d, $J = 16.4$ Hz, 1H), 4.04 (d, $J = 17.2$ Hz, 1H), 3.77 (s, 3H), 3.73 (s, 9H), 3.71 (s, 3H), 3.71 (s, 3H), 3.69 (s, 3H), 3.65 (s, 3H), 3.29 (dd, $J = 16.3, 5.9$ Hz, 1H), 3.14 (dd, $J = 16.2, 3.0$ Hz, 1H); $^{13}\text{C NMR}$ (75 MHz, DMSO) δ 153.5, 152.8, 149.2, 148.4, 140.2, 139, 133.1, 132.4, 119.1, 119.0, 112.3, 110.8, 108.4, 104.8, 104.7, 61.0, 60.7, 56.6, 56.4, 56.0, 56.0, 38.3; MS (ESI) m/z 576 $[\text{M} + \text{Na}]^+$; HRMS: calcd for $\text{C}_{30}\text{H}_{35}\text{NNaO}_9$ $[\text{M} + \text{Na}]^+$ 576.2210, found 576.2215; elemental calcd C, 65.09; H, 6.37; N, 2.53 for $\text{C}_{30}\text{H}_{35}\text{NO}_9$; found C, 64.95; H, 6.11; N, 2.73%.

N-(4-Methoxybenzoyl)-3-(3,5-Dimethoxyphenyl)-6,7,8-trimethoxy-1,2,3,4-tetrahydroisoquinoline (2m). The title compound was prepared from **9b** (125 mg, 0.34 mmol) and 4-methoxybenzoyl chloride **13a** (72 μL , 0.53 mmol) in a manner similar to that described for **2k**. The residue was purified by flash chromatography using 35% ethyl acetate in hexane to afford **2m** (38 mg, 22%) as white solid. mp (hexane) 55–56 °C; $^1\text{H NMR}$ (300 MHz, $\text{DMSO}-d_6$, 353 K) δ 7.39 (d, $J = 8.8$ Hz, 2H), 6.99 (d, $J = 8.8$ Hz, 2H), 6.69 (s, 1H), 6.33 (t, $J = 2.2$ Hz, 2H), 6.29 (s, 1H), 5.42 (bs, 1H), 4.80 (d, $J = 16.5$ Hz, 1H), 4.04 (d, $J = 17.1$ Hz, 1H), 3.79 (s, 3H), 3.77 (s, 3H), 3.69 (s, 3H), 3.66 (s, 9H), 3.33–3.17 (m, 2H); $^{13}\text{C NMR}$ (75 MHz, CDCl_3) δ 161.2, 161.0, 152.8, 147.8, 140.2, 130.5, 130.5, 129.3, 128.9, 121.7, 114.5, 108.3, 105.1, 98.9, 61.0, 56.5, 55.9, 55.7, 55.5, 32.9, 32.9; MS (ESI) m/z 494 $[\text{M} + \text{H}]^+$; HRMS: calcd for $\text{C}_{28}\text{H}_{32}\text{NO}_7$ $[\text{M} + \text{H}]^+$ 494.2179, found 494.2177; El. elemental calcd C, 68.14; H, 6.33; N, 2.84 for $\text{C}_{28}\text{H}_{31}\text{NO}_7$; found C, 67.95; H, 6.48; N, 2.60%.

N-(3,4,5-Trimethoxybenzoyl)-3-(3,5-Dimethoxyphenyl)-6,7,8-trimethoxy-1,2,3,4-tetrahydroisoquinoline (2n). The title compound was prepared from **9b** (125 mg, 0.34 mmol) and 3,4,5-trimethoxybenzoyl chloride **13b** (160 mg, 0.69 mmol) in a manner similar to that described for **2k**. The residue was purified by flash chromatography using 35% ethyl acetate in hexane to afford **2n** (29 mg, 25%) as white solid. mp (hexane) 150–152 °C; $^1\text{H NMR}$ (300 MHz, DMSO) δ 6.65 (s, 3H), 6.37–6.24 (m, 3H), 5.34 (bs, 1H), 4.83 (d, $J = 16.6$ Hz, 1H), 4.13 (d, $J = 17.1$ Hz, 1H), 3.76 (s, 6H), 3.71 (d, $J = 1.9$ Hz, 12H), 3.66 (s, 6H), 3.28 (dd, $J = 16.0, 5.6$ Hz, 1H), 3.18–3.03 (m, 1H); $^{13}\text{C NMR}$ (75 MHz, CDCl_3) δ 171.0, 161.1, 153.4, 152.7, 149.9, 143.8, 140.3, 139.0, 132.3, 129.1, 108.4, 105.1, 104.7, 99.1, 61.1, 61.0, 60.7, 56.4, 55.7, 39.3, 33.7; MS (ESI) m/z 576 $[\text{M} + \text{Na}]^+$; HRMS: calcd for $\text{C}_{30}\text{H}_{35}\text{NNaO}_9$ $[\text{M} + \text{Na}]^+$ 576.2210, found 576.2209; elemental calcd C, 65.09; H, 6.37; N, 2.53 for $\text{C}_{30}\text{H}_{35}\text{NO}_9$; found C, 65.21; H, 6.66; N, 2.75%.

Static protein adhesion assay

Preparation of recombinant protein ICAM-1-Fc and *Plasmodium falciparum* parasite line ItG culture were performed as described in ref. 25. Purified recombinant ICAM-1-Fc protein and PBS only (as negative control) were spotted in triplicate in a radial pattern using 2 μL spots on 60 \times 50 mm bacteriological plastic Petri dishes (Falcon 1007; Becton Dickinson, Oxford, UK) at concentrations of 50 $\mu\text{g mL}^{-1}$ for ICAM-1. This concentration

had previously been shown to be within the dynamic range for detecting differences in adhesion and produce coated surfaces with receptors at levels approximately equal to receptor densities seen on activated endothelium. The dishes were placed in a humidified chamber for 2 h at 37 °C to allow the proteins to adsorb to the surface of Petri dish, after which the protein solution and PBS were aspirated off and the uncoated plastic area was blocked overnight with 1% BSA/PBS at 4 °C. The plates were warmed at 37 °C for 1 h, blocking solution (1% BSA/PBS) was removed and plates were washed with binding buffer (RPMI 1640 with 2% glucose) prior to adding 1.5 mL of parasite culture (3% parasitaemia; 1% hematocrit in binding medium), with and without 50 μM of our compounds. The plates were incubated at 37 °C for 1 h with gentle resuspension every 10 min. Unbound infected and uninfected erythrocytes were removed by gentle manual washing (4–6 washes) with 2 mL binding medium per wash (monitoring of adhered cells was performed using an inverted microscope). The adhered iRBCs were fixed with 1% glutaraldehyde in phosphate buffered saline for 1 h and stained with 10% Giemsa for 30 minutes. Adhesion levels of all parasite strains (with and without our compounds) were quantified by microscopy using a unique, anonymous identifier for each dish (with the operator blinded to the iRBC category) and results were expressed as the mean number of iRBCs bound per mm² of surface area. The results were compared to quantify the effect of compounds on binding of ICAM-1 binding iRBCs to human ICAM-1.

Toxicity evaluation

NIH3T3 cell line was utilized for cytotoxicity experiments. NIH3T3 were maintained in DMEM and HepG2 in EMEM at 37 °C in a humidified atmosphere containing 5% CO₂. The culture media were supplemented with 10% fetal calf serum (FCS), 1% L-glutamine–penicillin–streptomycin solution, and 1% MEM nonessential amino acid solution. Once at confluence, cells were washed with 0.1 M PBS, taken up with trypsin–EDTA solution, and then centrifuged at 1000 rpm for 5 min. The pellet was resuspended in medium solution (dilution 1 : 15). Cell viability after 24 h of incubation with the different compounds was evaluated by Neutral Red Uptake (Sigma-Aldrich, Switzerland). The data processing included the Student's *t* test with *p* < 0.05 taken as significance level.

Computational details

All calculations performed in this work were carried out on Cooler Master Centurion 5 (Intel Core i5–2500 CPU @ 3.30 GHz Quad) with Ubuntu 10.04 LTS (long-term support) operating system running Maestro 9.2 (Schrödinger, LLC, New York, NY, 2011).

DBLβ–ICAM^{D1D2} complex generation

Homology modeling of PfEMP1–DBLβ domain. The sequence of *Plasmodium falciparum* PfEMP1 IT4VAR13 was taken in fasta format from the UniProtKB (entry A3R6S0; 3277AA).³⁶ The DBLβ domain information, relating to the sequence to be modeled was extracted from the above-mentioned full length

sequence according to the model recently published.²¹ The selection of templates was performed by means of HHpred web server (<http://www.toolkit.tuebingen.mpg.de/hhpred>).³⁷ Following this approach, three best templates with the higher sequence identity were identified and designated in order to build the 3D structure of the selected domain. The sequences of NTS-DBL1 domain of PFEMP1 (Protein Data Bank code 2XU0; sequence identity 31%; sequence similarity 60%), NTS-DBL1 and CIR-γ double domain of PFEMP1 (Protein Data Bank code 2YK0; sequence identity 31%; sequence similarity 60%), and DBL3x domain of PFEMP1 (Protein Data Bank code 3BQK; sequence identity 23%; sequence similarity 43%) were used as templates. After templates selection, Easy Modeller 3.0 and Modeller 9v10 package were used for modeling the DBLβ domain.^{38,39} Homology models were generated by means of a multiple templates-based homology modeling approach as previously reported by some of us for a different target.²⁸ We chose to make use of multiple templates in the modeling for increasing the quality of the obtained model.^{40,41} The models were scored and ranked on the basis of their DOPE (Discrete Optimized Potential Energy) score as calculated by the Modeller package. The best homology model obtained was imported into Schrödinger Maestro molecular modeling environment and then submitted to a refinement protocol in the Prime environment.^{33,42} In particular, we performed side-chain optimization with default settings and loop refinement using ultra extended in serial loop sampling options as recommended by means of Prime user manual for loops with 10 or more residues. Further structure optimization was carried out following two different approaches.

Method-1MM-PPW. DBLβ domain homology model minimization was performed by using MacroModel, and the Optimized Potentials for Liquid Simulations-all atom (OPLS-AA) force field 2005.^{43,44} The solvent effects were simulated using the analytical Generalized-Born/Surface-Area (GB/SA) model,⁴⁵ and no cutoff for non-bonded interactions was applied. Polak-Ribière Conjugate Gradient (PRCG) method⁴⁶ with 100 000 maximum iterations and a 0.001 gradient convergence threshold was employed. Moreover, the minimized DBLβ homology model was submitted to protein preparation wizard implemented in the Schrödinger suite 2011 (Protein Preparation Wizard workflow 2011; <http://www.schrodinger.com/supportdocs/18/16>). This protocol, through a series of computational steps, allowed us to obtain a reasonable starting structure of the protein for molecular docking calculations. In particular, we performed three steps to (1) add hydrogens, (2) optimize the orientation of hydroxyl groups, Asn, and Gln, and the protonation state of His, and (3) perform a constrained refinement with the impref utility, setting a maximum RMSD value of 0.30. The impref utility consists of cycles of energy minimization based on the impact molecular mechanics engine and on the OPLS_2005 force field.^{43,44}

Method-2 PPW-MM. In the second method MM minimization was performed after a first run of PPW.

The modeled protein was analyzed by generating a Ramachandran plot with the RAMPAGE webserver.⁴⁷ As shown in Figure S1,† 86.4% (335 amino acids) of protein residues were in the favored region of the plot, 13.1% (51 amino acids) of the

residues lay in an additional allowed region, and only 0.5% of the residues (2 amino acids not involved in the binding site) were located in the disallowed region. The results of RAMPAGE webserver revealed that over 99% of the residues of our DBL β domain refined model sat in the allowed regions of the Ramachandran Plot. This value is higher than the defined cut-off value (96.1%) for the most reliable models.⁴⁸ Consequently, the stereochemical quality of our DBL β domain homology model was found acceptable, displaying a very low percentage of residues having phi/psi angles in outlier regions.⁴⁷

Docking studies. Protein–protein docking calculation was performed by means of HADDOCK.³⁰ The developed protocol makes use of biochemical and/or biophysical interaction data such as chemical shift perturbation data, mutagenesis data, or molecular modeling predictions and thus incorporates structural knowledge of the target to drive the docking procedure.³⁰ Moreover, HADDOCK introduces the possibility to drive the selection step by identified data (experimental or computational) about the interacting regions of the proteins. This information is introduced as ambiguous interaction restraints (AIRs). The docking is then driven by a force that pulls the selected regions together. The calculation was performed with default parameters using the web server version of HADDOCK.²⁹ The residues of the DBL β domain potentially involved in the protein–protein interaction were defined from the output derived from SiteMap.³¹ In particular, the residues comprised in the predicted binding site calculated by SiteMap were considered as active. As reported in Fig. S3 of the ESI,[†] the active residues for docking calculation (represented by thin tube) are: C911, R913, R915, Y916, P918, I923, K1005, S1006, N1007, G1016, T1017, P1018, L1019, D1020, D1021, I1023, P1024, R1026, L1027, R1028, M1030, V1031, E1032, E1035, R1097, A1104, I1106, F1113, Y1120, Q1122, M1123, V1124, H1125. Concerning ICAM-1 interacting loop, the active residues involved in the docking calculation are L42–R49. After specification of the active regions of both proteins, passive residues were automatically defined around the active sites. The docking protocol consisted of three steps: (1) a rigid-body energy minimization, (2) a semi-flexible refinement by simulated annealing in torsional angle space, (3) a final refinement of each complex in explicit solvent (water) in order to improve the reliability of the model. After execution of these steps, the docked conformations are scored and ranked by the scoring function to facilitate the selection of the best conformations. The HADDOCK score takes into account the weighted sum of van der Waals (vdW), electrostatic, desolvation and restraint violation energies together with buried surface area. In this study the complex was chosen considering the better combination between the HADDOCK calculation scores and a visual inspection for finding the right complex orientation, according to the model presented by Brown and colleagues.²¹

Complex refinement. The selected model was superimposed to experimental SAXS data provided by Brown and colleagues²¹ by means of SUPCOMB.³² Distance constraints derived from experimental SAXS data were included in the minimization process using MacroModel.⁴⁹ The complex was minimized using OPLS_2005 as force field,^{43,44} GB/SA model⁴⁵ for

simulating the solvent effects and no cutoff for non-bonded interactions. The PRCG method with 100 000 maximum iterations and a 0.001 gradient convergence thresholds was employed. The output of this computational step is reported in Fig. 2 and S2.[†]

Structure-based pharmacophore generation

The DBL β –ICAM^{D1D2} complex was employed for a structure-based (SB) pharmacophore generation by means of the e-Pharmacophore application.³³ In order to obtain the starting structure, only the interaction loop of ICAM-1 was selected for this step, and the loop conformation obtained from the HADDOCK minimized complex was saved as .mae and used in Glide rigid docking.³⁵ The grid box was generated with default settings using the DE-loop as the centre of the box. Subsequently, the interacting loop (L42–L49) was docked in the same conformation derived from the complex generated by HADDOCK using Glide extra precision (XP) method. This method allows to generate a .Xpdes file containing the information about protein–ligand interaction, indispensable for developing a structure-based pharmacophore by means of e-Pharmacophore. The Glide pose was selected and used in e-Pharmacophore GUI. The ligand mode option was used to develop a pharmacophore hypothesis. The maximum feature option was set to 8, with a minimum inter-feature distance of 2.0 Å. Receptor-based excluded volumes were created using 0.5 as van der Waals scaling factor. Pharmacophore sites were automatically generated from the protein–ligand docked complex with Phase using the default set of six chemical features: hydrogen bond acceptor (A), hydrogen bond donor (D), hydrophobic (H), negative ionizable (N), positive ionizable (P), and aromatic ring (R);²⁷ no user-defined features were employed in this study. The e-Pharmacophore hypothesis was imported and managed into Phase according to docking studies. The obtained SB pharmacophore is reported in Fig. 4. The SB hypothesis consists of six features: two hydrogen-bond acceptors (A; represented by red vectors), two hydrogen bond donors (D; represented by light blue vectors), one hydrophobic function (H; represented by a green sphere) and one positive ionizable centre (blue sphere). The distance between selected AADDHP features is reported in Fig. S5 of the ESI.[†] The fitness evaluation of selected compounds was performed by means of Phase,²⁷ applying the “find matches” method using the existent conformers for each compound previously generated by MacroModel (see the ligand preparation paragraph for further details);⁴⁹ in the hit treatment panel “apply excluded volumes” was selected for calculating the fitness. The outcome is reported in Table 1, while the superposition between all compounds in the study (1; 2a–n) and AADDHP pharmacophore is reported in Fig. 4 of the Main Text and in Table S2 of the ESI.[†]

Ligand preparation

Three-dimensional structures of all compounds in this study were built by means of Maestro 9.2.³³ Conformers of each derivative were generated by MacroModel using the Optimized Potentials for Liquid Simulations-all atom (OPLS-AA) force field

2005.^{43,44,49} The solvent effects are simulated using the analytical Generalized-Born/Surface-Area (GB/SA) model,⁴⁵ and no cutoff for nonbonded interactions was selected. Molecular energy minimizations were performed using the Polak-Ribiere conjugate gradient (PRCG)⁴⁶ method with 1000 maximum iterations and a 0.001 gradient convergence threshold. Conformational searches were carried out by application of the MCMM (Monte Carlo Multiple Minimum) torsional sampling method, performing an automatic setup with 20 kJ mol⁻¹ in the energy window for saving structure and a 0.5 Å cutoff distance for redundant conformers.

Acknowledgements

P. R. P. was funded by the European Union Framework Programme 7-Marie Curie FP7 programme, under grant agreement no. PITN-GA-2008-215281. Authors wish to thank Schrodinger LLC, NY and S-IN for providing the trial version of e-Pharmacophore application. Authors wish to thank the Italian Ministry of University and Research (Project PRIN MIUR n° 200925BPZ5_002) for financial support.

Notes and references

- 1 WHO World Malaria Report 2012, http://www.who.int/malaria/publications/world_malaria_report_2012/en/ (20/08/2013).
- 2 H. C. van der Heyde, J. Nolan, V. Combes, I. Gramaglia and G. E. Grau, *Trends Parasitol.*, 2006, **22**, 503–508.
- 3 G. D. Turner, H. Morrison, M. Jones, T. M. Davis, S. Looareesuwan, I. D. Buley, K. C. Gatter, C. I. Newbold, S. Pukritayakamee, B. Nagachinta, *et al.*, *Am. J. Pathol.*, 1994, **145**, 1057–1069.
- 4 E. Pongponratn, G. D. Turner, N. P. Day, N. H. Phu, J. A. Simpson, K. Stepniewska, N. T. Mai, P. Viriyavejakul, S. Looareesuwan, T. T. Hien, D. J. Ferguson and N. J. White, *Am. J. Trop. Med. Hyg.*, 2003, **69**, 345–359.
- 5 S. J. Chakravorty, K. R. Hughes and A. G. Craig, *Biochem. Soc. Trans.*, 2008, **36**, 221–228.
- 6 A. R. Berendt, D. L. Simmons, J. Tansey, C. I. Newbold and K. Marsh, *Nature*, 1989, **341**, 57–59.
- 7 L. Turner, T. Lavstsen, S. S. Berger, C. W. Wang, J. E. Petersen, M. Avril, A. J. Brazier, J. Freeth, J. S. Jespersen, M. A. Nielsen, P. Magistrado, J. Lusingu, J. D. Smith, M. K. Higgins and T. G. Theander, *Nature*, 2013, **498**, 502–505.
- 8 A. Mbengue, X. Y. Yam and C. Braun-Breton, *Br. J. Haematol.*, 2012, **157**, 171–179.
- 9 J. D. Smith, C. E. Chitnis, A. G. Craig, D. J. Roberts, D. E. Hudson-Taylor, D. S. Peterson, R. Pinches, C. I. Newbold and L. H. Miller, *Cell*, 1995, **82**, 101–110.
- 10 X. Z. Su, V. M. Heatwole, S. P. Wertheimer, F. Guinet, J. A. Herrfeldt, D. S. Peterson, J. A. Ravetch and T. E. Wellems, *Cell*, 1995, **82**, 89–100.
- 11 M. Avril, A. K. Tripathi, A. J. Brazier, C. Andisi, J. H. Janes, V. L. Soma, D. J. Sullivan, Jr, P. C. Bull, M. F. Stins and J. D. Smith, *Proc. Natl. Acad. Sci. U. S. A.*, 2012, **109**, E1782–E1790.
- 12 A. Claessens, Y. Adams, A. Ghumra, G. Lindergard, C. C. Buchan, C. Andisi, P. C. Bull, S. Mok, A. P. Gupta, C. W. Wang, L. Turner, M. Arman, A. Raza, Z. Bozdech and J. A. Rowe, *Proc. Natl. Acad. Sci. U. S. A.*, 2012, **109**, E1772–E1781.
- 13 C. Gray, C. McCormick, G. Turner and A. Craig, *Mol. Biochem. Parasitol.*, 2003, **128**, 187–193.
- 14 C. Newbold, P. Warn, G. Black, A. Berendt, A. Craig, B. Snow, M. Msobo, N. Peshu and K. Marsh, *Am. J. Trop. Med. Hyg.*, 1997, **57**, 389–398.
- 15 L. B. Ochola, B. R. Siddondo, H. Ocholla, S. Nkya, E. N. Kimani, T. N. Williams, J. O. Makale, A. Liljander, B. C. Urban, P. C. Bull, T. Szeszak, K. Marsh and A. G. Craig, *PLoS One*, 2011, **6**, e14741.
- 16 J. Bella, P. R. Kolatkar, C. W. Marlor, J. M. Greve and M. G. Rossmann, *Proc. Natl. Acad. Sci. U. S. A.*, 1998, **95**, 4140–4145.
- 17 M. T. Tse, K. Chakrabarti, C. Gray, C. E. Chitnis and A. Craig, *Mol. Microbiol.*, 2004, **51**, 1039–1049.
- 18 S. M. Kraemer and J. D. Smith, *Curr. Opin. Microbiol.*, 2006, **9**, 374–380.
- 19 T. S. Rask, D. A. Hansen, T. G. Theander, A. Gorm Pedersen and T. Lavstsen, *PLoS Comput. Biol.*, 2010, **6**, e1000933.
- 20 J. D. Smith, G. Subramanian, B. Gamain, D. I. Baruch and L. H. Miller, *Mol. Biochem. Parasitol.*, 2000, **110**, 293–310.
- 21 A. Brown, L. Turner, S. Christoffersen, K. A. Andrews, T. Szeszak, Y. Zhao, S. Larsen, A. G. Craig and M. K. Higgins, *J. Biol. Chem.*, 2013, **288**, 5992–6003.
- 22 J. Gullingsrud, T. Saveria, E. Amos, P. E. Duffy and A. V. Oleinikov, *PLoS One*, 2013, **8**, e61323.
- 23 A. Bengtsson, L. Joergensen, T. S. Rask, R. W. Olsen, M. A. Andersen, L. Turner, T. G. Theander, L. Hviid, M. K. Higgins, A. Craig, A. Brown and A. T. Jensen, *J. Immunol.*, 2013, **190**, 240–249.
- 24 M. Dormeyer, Y. Adams, B. Kramer, S. Chakravorty, M. T. Tse, S. Pegoraro, L. Whittaker, M. Lanzer and A. Craig, *Antimicrob. Agents Chemother.*, 2006, **50**, 724–730.
- 25 P. R. Patil, S. Gemma, G. Campiani and A. G. Craig, *Malar. J.*, 2011, **10**, 348.
- 26 K. Ohmori, T. Yano and K. Suzuki, *Org. Biomol. Chem.*, 2010, **8**, 2693–2696.
- 27 *Phase, version 3.3, User Manual*, Schrödinger press, LLC, New York, NY, 2011.
- 28 A. Cappelli, M. Manini, S. Valenti, F. Castriconi, G. Giuliani, M. Anzini, S. Brogi, S. Butini, S. Gemma, G. Campiani, G. Giorgi, L. Mennuni, M. Lanza, A. Giordani, G. Caselli, O. Letari and F. Makovec, *Eur. J. Med. Chem.*, 2013, **63**, 85–94.
- 29 S. J. de Vries, M. van Dijk and A. M. Bonvin, *Nat. Protoc.*, 2010, **5**, 883–897.
- 30 C. Dominguez, R. Boelens and A. M. Bonvin, *J. Am. Chem. Soc.*, 2003, **125**, 1731–1737.
- 31 *SiteMap, version 2.5*, Schrödinger, LLC, New York, NY, 2011.
- 32 M. B. Kozin and D. I. Svergun, *J. Appl. Crystallogr.*, 2001, **34**, 33–41.
- 33 *Maestro, version 9.2*, Schrödinger, LLC, New York, NY, 2011.
- 34 N. K. Salam, R. Nuti and W. Sherman, *J. Chem. Inf. Model.*, 2009, **49**, 2356–2368.

- 35 *Glide, version 5.7*, Schrödinger, LLC, New York, NY, 2011.
- 36 M. Magrane and U. Consortium, *Database Oxford*, 2011, vol. 2011, bar009.
- 37 J. Soding, *Bioinformatics*, 2005, **21**, 951–960.
- 38 B. K. Kuntal, P. Aparoy and P. Reddanna, *BMC Res. Notes*, 2010, **3**, 226.
- 39 N. Eswar, D. Eramian, B. Webb, M. Y. Shen and A. Sali, *Methods Mol. Biol.*, 2008, **426**, 145–159.
- 40 N. Fernandez-Fuentes, B. K. Rai, C. J. Madrid-Aliste, J. E. Fajardo and A. Fiser, *Bioinformatics*, 2007, **23**, 2558–2565.
- 41 P. Larsson, B. Wallner, E. Lindahl and A. Elofsson, *Protein Sci.*, 2008, **17**, 990–1002.
- 42 *Prime, version 3.0*, Schrödinger, LLC, New York, 2011.
- 43 W. L. Jorgensen, D. S. Maxwell and J. TiradoRives, *J. Am. Chem. Soc.*, 1996, **118**, 11225–11236.
- 44 G. A. Kaminski, R. A. Friesner, J. Tirado-Rives and W. L. Jorgensen, *J. Phys. Chem. B*, 2001, **105**, 6474–6487.
- 45 W. C. Still, A. Tempczyk, R. C. Hawley and T. Hendrickson, *J. Am. Chem. Soc.*, 1990, **112**, 6127–6129.
- 46 E. Polak and G. Ribiere, *Rev. Fr. Inform. Rech. Operation.*, 1969, **16-R1**, 35–43.
- 47 S. C. Lovell, I. W. Davis, W. B. Arendall, 3rd, P. I. de Bakker, J. M. Word, M. G. Prisant, J. S. Richardson and D. C. Richardson, *Proteins*, 2003, **50**, 437–450.
- 48 R. Luthy, J. U. Bowie and D. Eisenberg, *Nature*, 1992, **356**, 83–85.
- 49 *MacroModel. Version 9.9*, Schrödinger, LLC, New York, NY, 2011.